Aggregation of Dipalmitoylphosphatidylcholine Vesicles†

Martin Wong and T. E. Thompson*

ABSTRACT: Quasi-elastic and 90° light scattering were used to study the aggregation of dipalmitoylphosphatidylcholine vesicles at temperatures below the gel–liquid-crystalline phase transition as a function of concentration, temperature, and size. Increased vesicle concentration did not appreciably change aggregate size but did change the total number of aggregates in a manner consistent with a bimolecular collisional mechanism for the conversion of aggregates to fused vesicles. Increased temperature decreased aggregation, indicating that the disaggregation rate constant increased faster than the aggregation rate constant. As a function of size, aggregation decreasedly slightly from small to 700 Å diameter vesicles and increased considerably for 950 Å diameter vesicles. A model of the interaction of small vesicles below the the gel–liquid-crystalline phase transition is presented in which aggregation precedes fusion and collision between aggregates triggers fusion.

The preceding paper (Wong et al., 1982) and studies by Suurkuusk et al. (1976), Schullery et al. (1980), Lichtenberg et al. (1981), and Schmidt et al. (1981) showed that small vesicles about 200 Å in diameter formed from dipalmitoylphosphatidylcholine (DPPC)[1] fuse below the phase transition temperature (T_m = 41.6 °C) to 700 Å diameter vesicles and these further fuse to 950 Å diameter vesicles. The initial rate of fusion is approximately second order in concentration, a result also found for phosphatidylserine small vesicle fusion in the presence of Ca^{2+} (Wilschut et al., 1980). Several factors including concentration, temperature, and hydrocarbon chain length alter the initial rate of vesicle fusion but do not change the size of the fusion products.

The order of the fusion process suggests a bimolecular collisional mechanism, but the increased fusion rate with decreased temperature argues against simple vesicle–vesicle collision being the rate-limiting step. Also the small vesicle to 700 Å diameter vesicle conversion, with no appreciable intermediate sized material, indicates that approximately 18 small vesicles participate in the size-determining vesicle fusion step.

In this paper we investigate the aggregation of small, 700 Å diameter, and 950 Å diameter fused DPPC vesicles at temperatures below T_m as a function of time and relate the events of aggregation to the subsequent fusion process. At 4 °C in the vesicle concentration range 0.5–5 mM (P_i),[1] small vesicles aggregate and the size of the aggregates increases linearly with time. In the concentration range 20–120 mM (P_i), small vesicle aggregation is followed by fusion.

A model is developed in which aggregation precedes fusion and the collision of aggregates triggers the fusion event. Using small vesicle aggregation data taken below the phase transition and the theory for diffusion in a field of force (von Smoluchowski, 1917; Fuchs, 1934; Verwey & Overbeek, 1948; Spielman, 1970) together with the expression for the energy of interaction between vesicles derived from multilamellar liposome data (Lis et al., 1982), we estimate that small vesicles aggregate at a vesicle–vesicle separation distance of less than 5.2 Å.

Interest in this aggregation process derives primarily from the fact that vesicle aggregation is a necessary condition for vesicle fusion which generates unilamellar vesicles of large radius. It is these large vesicles that are of prime interest as bilayer systems modeling biological membrane bilayers and as drug delivery vehicles (Wong et al., 1982).

Materials and Methods

Quasi-Elastic Light-Scattering Measurements. Quasi-elastic light-scattering (QELS)[1] diameter was measured in a Model HN 5-90 laser-scattering spectrometer and a Model 6864 computing autocorrelator (Nicomp Instruments). Channel width was adjusted to give between 1.3 and 1.8 decays over the 56 channels. Approximately 2×10^7 correlated counts were accumulated per measurement, then the ln of the autocorrelation function was least-squares fitted with a cubic polynomial, and the distribution function of the decay rates was characterized by using the method of cumulants (Koppel, 1972). The Stokes radius [$R = KT/(6\pi\eta D)$] of the equivalent sphere was calculated from the diffusion coefficient D, using the appropriate temperature values of viscosity (η) and index of refraction for water (*Handbook of Physics and Chemistry*, 1970–1971; *International Critical Tables*, 1930). At the lipid concentrations used, corrections to the index of refraction were less than 1% (Yi & MacDonald, 1973; Chong & Colbow, 1976) and did not significantly change the results. The diameters of fused vesicles of initial molar phospholipid concentration below 20 mM (P_i) were measured directly, while higher concentration samples were diluted into buffer and then suspended by vortexing prior to measurement. Calibration measurements were made with uniform polystyrene latex beads [1000 (±80) (Polysciences), 910 (±58), and 380 (±75) Å diameter (Dow Chemical Co.)] and with small sonicated vesicles [about 240-Å diameter (Mason & Huang, 1978)] prepared from 1-palmitoyl-2-oleoylphosphatidylcholine according to Barenholz et al. (1977). The QELS diameters were approximately 4.7% higher than manufacturer's mean diameters, but within the stated standard deviation. The laser wavelength was 632.8 nm. The sample chamber was temperature regulated to ±0.1 °C.

Light Scattering at 90°. Relative 90° scattered light intensity was measured in an SLM 4800 (SLM Instruments) with both the incident and emission monochromators at 589 nm. The sample chamber was temperature regulated to ±0.1

† From the Department of Biochemistry, University of Virginia School of Medicine, Charlottesville, Virginia 22908. *Received September 9, 1981; revised manuscript received May 7, 1982.* This investigation was supported by U.S. Public Health Service Grants GM-14628 and GM-23573. M.W. was supported by NRSA Postdoctoral Fellowship GM-07463.

[1] Abbreviations: DPPC, dipalmitoylphosphatidylcholine; QELS, quasi-elastic light scattering; Pipes, piperazine-*N*,*N*′-bis(2-ethanesulfonic acid); (P_i), concentration of inorganic phosphate; RGD, Rayleigh–Gans–Debye.

0006-2960/82/0421-4133$01.25/0

°C and flushed with dry N_2. Sample cuvettes were covered with Teflon caps. Both polarizers were set at 55°. The relation between 90° scattered light intensity and the polarizer angle, $I(55/55) = I(0/0) \cos^2(55)$ (Jonker, 1952), was tested and found to be well obeyed. Measurements were made in the A/B mode with a reference solution of 0.25 mg/mL glycogen in the B channel. Glycogen was dispersed with a bath sonicator and prepared daily. The system gain was adjusted to 0.05 with reference solution also in the A channel. For aggregation studies the vesicles at 50 °C were added to cuvettes equilibrated at 4 °C. Dilutions were checked by measuring inorganic phosphate (Bartlett, 1959).

Preparation of Vesicles. (A) Small sonicated vesicles were prepared from 1,2-dipalmitoyl-*sn*-phosphatidylcholine (DPPC) (Huang, 1969; Barenholz et al., 1977). The sample was kept at 50 °C in 20 mM Pipes (pH 7.4), 10 mM NaCl, and 0.02% NaN_3. Following sonication, the vesicles were centrifuged for 30 min at 100000*g* to remove probe particles and then for 60 min at 100000*g* to separate the small vesicle component. For QELS, only the very top 10% material was then carefully removed with a 20-μL pipetman. Small sonicated vesicles were prepared at high concentration [100–120 mM (P_i)], and lower concentration samples were obtained by dilution with buffer and suspension by vortexing. A control sample of small vesicles was incubated at 50 °C in a Teflon tape-covered glass test tube, which contained no air space.

(B) Fractionated, fused 700 Å diameter vesicles were prepared by cooling small sonicated DPPC vesicles (made at 50 °C) to 21 °C. After 10 days the vesicles were fractionated on a Sepharose CL-2B column, and the fractions from the fused vesicle peak were pooled (Schullery et al., 1980).

(C) Fused 950 Å diameter vesicles were prepared from small DPPC vesicles sonicated at 120 mM (P_i) at 50 °C and then incubated at 4 °C for more than 35 days (Wong et al., 1982). Vesicles were stored at 4 °C until needed. An aliquot of this stock dispersion was diluted into buffer to the desired concentration and vortexed to suspend the sample.

Disaggregation of Vesicles by Heating. Aggregated vesicles were prepared from small sonicated DPPC vesicles diluted to 5 mM (P_i) and then cooled to 4 °C. (A) After 49 h the sample was hand shaken to suspend the sample, and the QELS radius of an aliquot was measured as a function of increasing temperature. The temperature was increased in steps, and the aliquot was allowed to equilibrate 10–20 min prior to each measurement. (B) After 6-days incubation at 4 °C, the sample was hand shaken, and an aliquot was diluted to 0.56 mM (P_i) in order to monitor 90° light-scattering intensity as a function of temperature. Temperature was scanned up from 4 °C at 20 °C/h to above T_m and then down again to 4 °C. The sample was stirred continuously, and both polarizers were set to vertical.

Results and Discussion

QELS Measurements on Mixed Populations of Vesicles of Known Sizes. The QELS diameter of well-defined mixtures was measured in order to be able to interpret the QELS diameter measurements of 208, 700, and 950 Å diameter vesicles during fusion. QELS diameter as a function of the percent total lipid in the larger vesicles of binary mixtures is shown in Figure 1A for mixtures of 208 ± 31 and 768 ± 7 Å diameter vesicles and in Figure 1B for mixtures of 782 ± 6 and 1172 ± 18 Å diameter vesicles. The results demonstrate the weighting toward the larger particles in binary mixtures seen in QELS measurements. When 20% of the lipid was in 700-Å vesicles, the QELS diameter was 700 Å (Figure 1A). When 50% of the lipid was in 950 Å diameter vesicles, the QELS diameter was 950 Å (Figure 1B). When the abscissa is expressed in numbers of vesicles, the weighting is even more pronounced, since approximately 18 small vesicles have the same number of lipid molecules as one 700 Å diameter vesicle and approximately two 700 Å diameter vesicles have the same number as one 950 Å diameter vesicle.

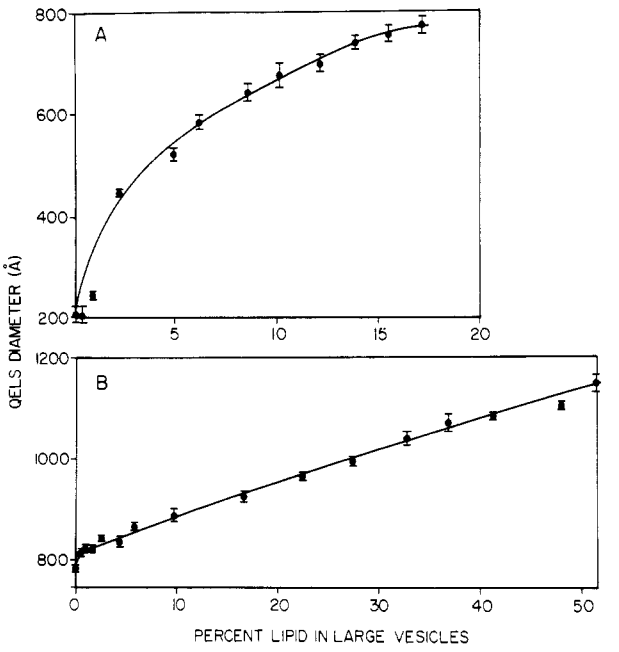

FIGURE 1: (A) Binary mixtures of 208 ± 31 Å 1-palmitoyl-2-oleoylphosphatidylcholine small sonicated vesicles and 768 ± 7 Å DPPC fused vesicles, where the diameters are the mean and the standard deviation of five QELS measurements, at 50 °C. The curves were constructed by adding between 10- and 50-μL aliquots of the larger vesicles [10.3 mM (P_i)] to 0.3 mL of small vesicles [60 mM (P_i)]. Samples were vortexed and allowed to temperature equilibrate before reading. Measurements were in buffer (20 mM Pipes, 10 mM NaCl, and 0.02% NaN_3). (B) Binary mixtures of 782 ± 6 Å and 1172 ± 18 Å DPPC fused vesicles. Between 10- and 40-μL aliquots of larger vesicles [2.5 mM (P_i)] were added to 0.3 mL of smaller vesicles [10.3 mM (P_i)]. The remaining conditions were the same as above.

These results are consistent with the results obtained by Briggs & Nicoli (1980) who have addressed the problem of intensity weighting for a polydisperse system of spherical particles which have the same uniform polarizability. These workers weighted the first-order correlation function by $N_j(V_j\beta_jG_j)^2$ for N_j particles of diffusion coefficient D_j, where V_j is the particle volume, β_j is the polarizability factor, and G_j is the spherical particle form factor. The correlation function was reduced by using the method of cumulants (Koppel, 1972). Experimental studies by Briggs & Nicoli (1980) on binary mixtures of uniform latex spheres gave results in good agreement with the calculated weighted curve and demonstrated the intensity weighting of the QELS diameter toward the larger particles in a polydisperse system. These results and the data shown in Figure 1 indicate that when following aggregation with QELS, the increased diameter may only be indicative of the size of a subpopulation of larger particles. On the other hand, when following disaggregation, return of the QELS diameter to the original value is a good indication that very few large particles are present.

QELS Measurement on Small Vesicles as a Function of Time. Figure 2 shows the QELS diameter as a function of time for small vesicle dispersions. The lowest curve in Figure 2, obtained for vesicles at 50 °C, clearly shows that vesicle size was invariant for at least 47 h. In contrast to this result, at 4 °C the QELS diameter increased with time as is shown

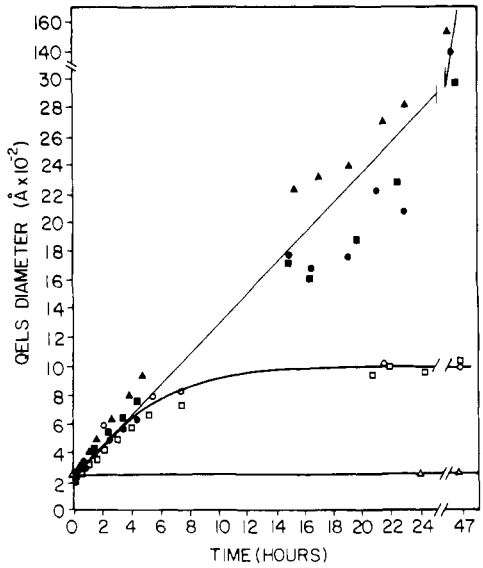

FIGURE 2: QELS diameter as a function of time. Small sonicated DPPC vesicles at 112 (○), 20 (□), 5 (▲), 1 (●), and 0.25 mM (P_i) (■) were formed at 50 °C and then cooled to 4 °C at $t = 0$. Small sonicated vesicles [20 mM (P_i) in 100 mM KCl and 0.02% NaN_3] kept at 50 °C (▲). Points are the mean of four measurements.

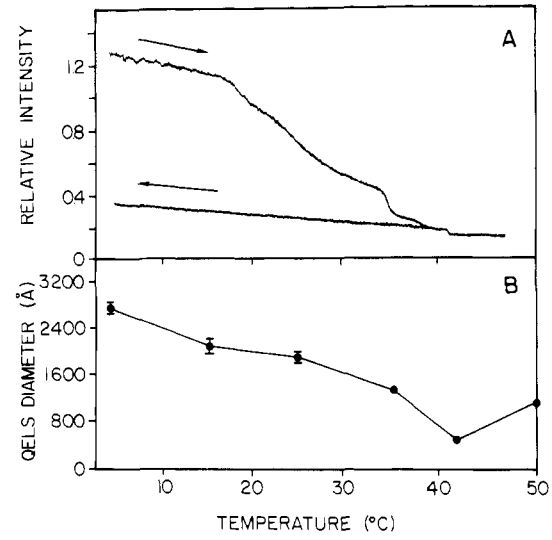

FIGURE 3: Disaggregation by heating of small sonicated vesicles aggregated at 4 °C and 5 mM (P_i) (A) 90° scattered light vs. temperature for a 6-day aggregated sample heated to 47 °C and then cooled to 4 °C. (B) QELS diameter vs. temperature for a 49-h aggregated sample heated in step increments from 4 °C.

by the upper two curves in Figure 2. During the initial 4 h the QELS diameter increased linearly with time and, to a first approximation, independently of concentration. Beyond 4 h, however, the QELS diameter, obtained at higher vesicle concentrations [20–112 mM (P_i)] and shown in the middle curve, gradually reached a plateau value of 950–1000 Å after 24–48 h. The particles formed under these conditions have been shown by a variety of methods to be large unilamellar vesicles which apparently are formed by the fusion of aggregated vesicles (Wong et al., 1982). For this to be the case, it is necessary for the time course of aggregation of vesicles to be faster than the time course of fusion. That this in fact occurs can be seen by comparing the time course of the QELS diameter increase, which reflects both fusion and aggregation, with the time course of fusion alone as assessed by Sepharose CL-2B molecular sieve chromatography in the preceding paper (Wong et al., 1982). For example, at 7.5 h the Sepharose CL-2B column profiles contained 8% 700 Å diameter fused vesicles and 92% small vesicles, which from Figure 1A (for 700-Å and unaggregated small vesicles) should give a QELS diameter of 620 Å. In Figure 2, the QELS diameter is 720 Å at this time. Therefore the small vesicles were aggregated, in addition to being approximately 8% fused. In Figure 2, the QELS diameter was 950 Å for incubation times greater than 1 day. From Sepharose CL-2B column profiles, the 7-day incubated sample (120 mM (P_i)) contained only 700 Å diameter vesicles. Therefore the QELS diameter at 7 days was the result of aggregation of 700-Å vesicles. Sepharose CL-2B column profiles showed that the aggregated 700-Å vesicles fused to 950 Å diameter vesicles after 35 days.

Beyond 4 h, at lower vesicle concentrations [0.5–5 mM (P_i)], shown in the upper curve of Figure 2, the QELS diameter continued to increase linearly for at least 24 h. Evidence that this linear increase in QELS diameter is due for the most part to aggregation of small vesicles and not to fusion is presented in Figure 3. The upper curve in Figure 3A is the 90° scattered light intensity as a function of temperature and shows a monotonic decrease with increasing temperature. Changes in slope were found at approximately the DPPC subtransition temperature, 17 °C (Chen et al., 1980), and the pretransition temperature, 34 °C, noted in multilamellar structures. The slope change at the transition temperature, 41 °C, was due to the change in the index of refraction which occurs at the gel–liquid-crystalline phase transition as described by Yi & MacDonald (1973) and Chong & Colbow (1976). A control sample kept at 50 °C (♦) gave a relative intensity slightly less than the disaggregated sample. The lower curve in Figure 3A is the cooling scan of the disaggregated vesicles. Only the change in the index of refraction at the transition temperature is seen since the time course of reaggregation is much longer than the 3 h required for the scan. Figure 3B is the QELS diameter as a function of temperature and shows a monotonic decrease from 2780 ± 120 Å at 4 °C to 510 ± 6 Å at 42 °C. Complete disaggregation to small vesicles would have been to a diameter of 240 Å.

From the light-scattering data, we cannot determine whether the sample at 42 °C was composed of mostly 510 Å diameter structures or was small vesicles with a few larger aggregates. It is clear, however, that the QELS diameter at low concentrations (in Figure 2) was due to aggregates which can be heat dissociated to much smaller structures. The QELS diameter showed an increase when the temperature was raised from 42 to 50 °C, due to aggregation above the phase transition temperature seen in unstirred samples. This was not seen with 90° light scattering (Figure 3A) with samples which were stirred while heating. Aggregation of samples heated above the phase transition temperature is presently under investigation.

Further evidence that the upper curve in Figure 2 is due for the most part to aggregation and not fusion is presented in the freeze–fracture electron micrograph in Figure 4. This was a sample of small vesicles [5 mM (P_i)] incubated at 4 °C for 18 h. The sample consisted of aggregates plus some small vesicles and fused vesicles. In contrast, electron micrographs of samples corresponding to the middle curve in Figure 2 (high vesicle concentrations) showed small and 700 Å diameter fused vesicles, with few aggregates (Wong et al., 1982).

Light-Scattering Measurements at 90° on Small Vesicles as a Function of Time. The initial aggregation at 4 °C was also monitored by 90° light scattering. Figure 5A is the relative intensity vs. time for small DPPC vesicles cooled to 4 °C. The rapid changes seen during the first 5 min are due to the change in the index of refraction as the samples cooled.

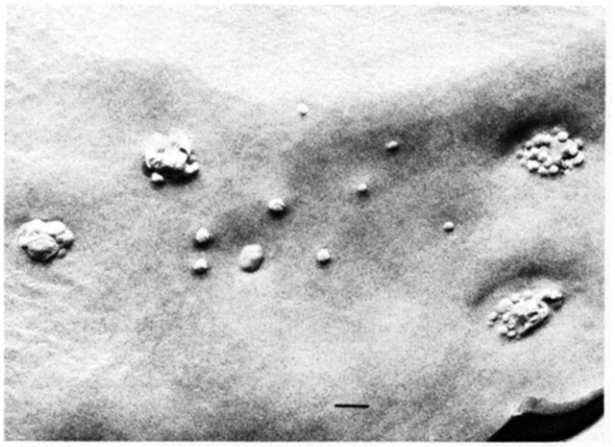

FIGURE 4: Freeze–fracture electron micrograph of small sonicated vesicles [5 mM (P_i)] incubated at 4 °C for 18 h. The marker corresponds to 1000 Å.

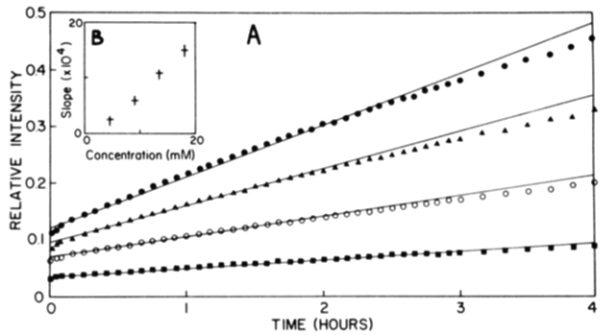

FIGURE 5: 90° scattered light intensity vs. time for aggregating small vesicles at 4 °C [(●) 18, (▲) 13.5, (○) 9, and (■) 4.5 mM (P_i)]. The straight lines are linear regressions to the data points from 5 min to 2 h, and the correlation coefficients were greater than 0.9997. The experimental half-times were 159 [18 mM (P_i)], 177 [13.5 mP (P_i)], 229 [9 mM (P_i)], and 306 min [4.5 mM (P_i)] extrapolated from the linear regressions (see text). (B) Slope (from the linear regressions in Figure 4A) vs. concentration.

The straight lines are linear regressions to the data points from 5 min to 2 h, and the slope vs. concentration is given in Figure 5B. The slope is an approximately linear function of concentration over the range 4.5–18 mM (P_i). Lansman & Haynes (1975) also found an approximately linear relation between the rate of scattered light increase and vesicle concentration for phosphatidic acid vesicle aggregation in the presence of $CaCl_2$.

The problem of light scattering from a diffusion-limited irreversibility aggregating system of spheres subject to a short-range attractive force was considered by Lips et al. (1971), who calculated the Rayleigh-Gans–Debye (RGD)[1] form factors for combinations of linear, planar, and close-packed three-dimensional aggregates. The RGD form factors were then used together with the scattering function from Mie theory for spherical phospholipid shells (Tinker, 1972; Oster & Riley, 1952; Kerker, 1969; Chong & Colbow, 1976; Yi & MacDonald, 1973) and incorporated in the second-order collisional theory of von Smoluchowski (1917). The curves obtained by Lips et al. (1971) for the aggregation of polystyrene spheres were in good agreement with the predictions of fast aggregation theory. In contrast, the shapes of the curves in Figure 5A are in qualitative agreement, but the time course is markedly slower.

Quantitative estimates of the half-times characteristic of the data in Figure 5A can be made following the suggestion of Overbeek (1952) that the experimental half-time is the time for the 90° scattered light intensity to reach 3 times the original intensity. Experimental half-times of approximately 160–310 min were obtained by extrapolating a straight line through the data in Figure 5A obtained over the first 2 h. In contrast to this range of experimental half-times, the diffusion-limited half-time based on the fast aggregation theory is in the range (4–16) × 10^{-5} s. This number is calculated as follows: In fast aggregation theory the diffusion-limited half-time is $t_{1/2} = 1/(8\pi DRn_0)$ (von Smoluchowski, 1917), where D is the diffusion coefficient of small vesicles of radius R and n_0 is the initial vesicle concentration. The range of theoretical half-times was calculated for $D = 1.6 \times 10^{-7}$ cm^2 s^{-1}, $R = 133$ Å as determined from QELS data at 4 °C, and $n_0 = 4.5$–18 mM (P_i).

The ratio of the diffusion-limited aggregation half-time to the experimentally determined value α can be interpreted as the fraction of vesicle–vesicle collisions which lead to aggregation (von Smoluchowski, 1917). In our system $\alpha = (4\text{–}9) \times 10^{-9}$. An alternative interpretation relates $W = 1/\alpha$ to the effect on aggregation of vesicle diffusion in a field of force. From the theory of Fuchs (1934), Verwey & Overbeek (1948), and Spielman (1970)

$$W = 2\int_{2+h_0/a}^{\infty} \frac{D_{12}^{\infty}}{D_{12}} \exp\left(\frac{V}{KT}\right)\frac{ds}{s^2} \qquad (1)$$

where V is the potential energy of interaction, $s = 2a + h$ is the center to center distance between vesicles, h is the distance between vesicles (h_0 in the aggregated state), a is the vesicle radius, and D_{12}^{∞}/D_{12} is the correction for viscous interactions between the approaching vesicles.

The factor D_{12}^{∞}/D_{12} has been calculated by Spielman (1970) and increases faster than exponentially as vesicle separation decreases (from a value of about 2.0 at $h/a = 1.0$ to a value of about 6.9 at $h/a = 0.1$). The value of the potential energy of interaction V has not been measured for vesicles. However, V has been measured for the case of planar membranes in DPPC multilamellar liposomes by using an osmotic stress technique (Le Neveu et al., 1977; Parsegian et al., 1979) and has contributions from the repulsive "hydration" force and the attractive van der Waals force. To estimate V for vesicles, Lis et al. (1982) used the Derjaquin (1935) approximation to calculate the repulsive force between spheres and subtracted the van der Waals attraction between vesicles. For DPPC vesicles below the phase transition, V at small separations is dominated by the contribution from the hydration repulsion force and varies as $e^{-h/\lambda}$ where λ is on the order of 2 Å. At larger vesicle separations the hydration force is small, and the main contribution to V is from the longer ranged van der Waals attractive force. V has a minimum at 15–18 Å (about $-0.5KT$) and slowly increases to zero at large vesicle separations.

Equation 1 can be used to test the V calculated from multilayer data. Using W from the data in Figure 5A, D_{12}^{∞}/D_{12} from Spielman (1970), and V for DPPC at 25 °C from Lis et al. (1982), we calculated numerically the vesicle separation in the aggregated state, h_0, to be less than 10 Å. This value of h_0 is at a separation distance less than the minimum in the V curve and lies in a region where the vesicles are subject to a strong repulsive force. Therefore, the V curve derived from multilayer data requires modification in order to describe the potential interaction between aggregating vesicles so that the vesicles aggregate in a region where $\partial V/\partial s = 0$ (zero net force).

At large to moderate separation distances, the V curve derived from multilayer data is assumed to describe adequately

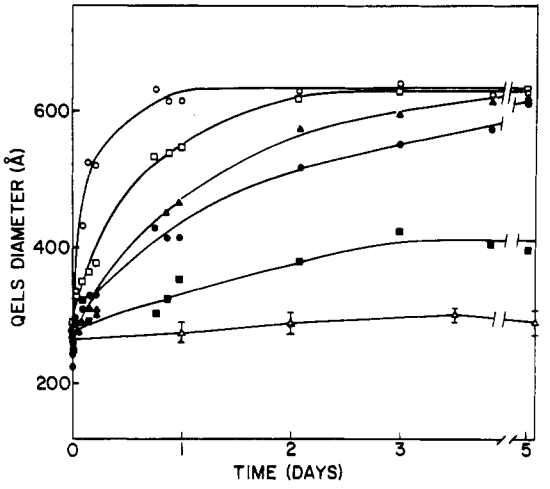

FIGURE 6: QELS diameter as a function of time. Small sonicated vesicles at 50 (○), 20 (□), 10 (▲), 5 (●), and 1 mM (P_i) (■) were formed at 50 °C and then cooled to 21 °C at $t = 0$. Small sonicated vesicles (20 mM (P_i) in 100 mM KCl and 0.02% NaN_3), kept at 50 °C (▲). Points are the mean of four measurements.

vesicle–vesicle interaction. At separation distances just below 10 Å, vesicle interaction is dominated by a hydration repulsive force of the form $e^{-h/\lambda}$ which prevents the vast majority of vesicle–vesicle encounters from approaching close enough to result in aggregate formation. For vesicle–vesicle encounters which result in aggregation, the simplest modification of V is one in which first a potential maximum and then a potential minimum ($\partial V/\partial s = 0$, at the h_0 separation distance) is encountered as vesicle–vesicle separation decreases beyond the region where the $e^{-h/\lambda}$ force dominates. The hydration repulsive force at small separations is attributed to the work required to remove water as the vesicle–vesicle separation distance decreases (Lis et al., 1982). A possible explanation for the modification of V into a maximum and minimum configuration at small vesicle–vesicle separations is that V changes as the vesicle deform when the number of water molecules separating the vesicles becomes small.

Equation 1 can be solved, by using V derived from multilayer data, for a value of h_0 which is an upper limit for the vesicle–vesicle separation distance in the aggregated state and for $V(h_0)$ which is an upper limit for the height of the potential energy maximum over which the vesicles pass during aggregation. The upper limits are $h_0 = 5.2$ Å and $V(h_0) = 19.7KT$.[2]

Temperature Dependence of Vesicle Aggregation. The data in Figure 3 show that increased temperature leads to net disaggregation of vesicles. A comparison of the data in Figure 6, QELS diameter vs. time for small vesicles incubated at 21 °C, with the 4 °C data in Figure 2 shows the rate at 21 °C to be at less than half the rate at 4 °C. In addition at 21 °C, the initial slope increases with vesicle concentration, in contrast to the distinct high and low concentration curves at 4 °C. A maximum value of about 640-Å diameter was found (compared to a maximum of about 1000-Å diameter, at 4 °C and high concentrations). Previously it was shown that a 20 mM (P_i) sample incubated for 3–5 days at 21 °C will contain both small and 700 Å diameter vesicles (Schullery et al., 1980). The maximum QELS diameter of 640 Å in Figure 6 shows that very few of the 700 Å diameter vesicles have aggregated since the QELS diameter detects larger structures with great sensitivity, as shown in Figure 1B. At 5 days, increasing the temperature to 50 °C did not decrease any of the QELS diameter readings. This observation is consistent with a low degree of aggregation of the 700 Å diameter fused vesicles. A control kept at 50 °C (lower curve) shows relatively little change in the QELS diameter over 5 days.

Figure 7 shows the aggregation of larger vesicles at various temperatures. In this figure the QELS diameter as a function of time is plotted for 950 Å diameter vesicles (A) and 700 Å diameter vesicles (B) equilibrated first at 50 °C for 1 h and then rapidly cooled to the measurement temperature. At the end of the incubations, heating the samples used in Figure 7A again to 50 °C produced nearly complete disaggregation. A similar result was obtained for the samples used in Figure 7B when they were reheated to 50 °C after several hours of incubation. It is clear that the degree of aggregation increased with decreasing temperature.

Second-order collisional rate theory predicts that aggregation should increase with increasing temperature since the collision rate increases with temperature (Nir et al., 1980). The data in Figures 3 and 7 show that this is certainly not the case for vesicle aggregation and further substantiate the idea discussed above that the rate of aggregation is not controlled by the collision rate. Day et al. (1980) found a similar temperature dependence for phosphatidylserine vesicle aggregation under conditions of high Na^+ concentration and negligible vesicle fusion.

Dependence of Aggregation Rate on Vesicle Size. An estimate of the dependence of the aggregation rate on vesicle diameter is seen in the initial slopes of the QELS diameter curves in Figure 2 and Figure 7. Normalizing the QELS diameter by dividing it by the vesicle diameter gives the initial slopes at 4 °C for small, 700 Å diameter, and 950 Å diameter vesicles equal to 0.4, 0.23, and 11.7 h^{-1}, respectively. Theory predicts that increased diameter will lead to decreased aggregation (Overbeek, 1977). This is seen in eq 1 where increased diameter increases the potential energy of interaction and therefore the entire integrand (Lis et al., 1982). Our estimates show an initial decrease and then a large increase in aggregation rate as the diameter increases.

A possible explanation for this size dependence is found in the relation between aggregation and the shape of the total potential energy interaction curve (Ottewill, 1973; Overbeek, 1977). Small DPPC vesicles aggregate at a distance between vesicle surfaces of less than 5.2 Å in the primary minimum. Small phosphatidylserine vesicles also aggregate in the primary minimum (Nir & Bentz, 1978). The large increase in aggregation rate for the 950 Å diameter vesicles may be due to their aggregation in the secondary minimum (Wiese & Healy, 1970; Nir et al., 1980). Calculations by Nir & Bentz (1978) show that aggregation in the secondary minimum is negligible for small vesicles but becomes significant for larger diameter vesicles.

Model of Aggregation and Fusion. Figure 8 depicts a model for the aggregation and fusion of DPPC vesicles at temperatures below the phase transition.

(I) Under conditions of low temperature and low concentration (Figure 2), aggregation increases as a function of time until the aggregates are so large that they settle to the bottom of the test tube. Bilayer–bilayer separation between aggregated vesicles is less than 5.2 Å, and the maximum in the potential energy of the interaction curve between aggregated small vesicles is less than $20KT$. Aggregation is largely reversible upon heating (Figure 3) and indicates that the disaggregation rate constant k'_d increases faster with temperature

[2] Calculated for 130 Å radius vesicles, a bilayer thickness of 35 Å, $P_0 = 10^{9.83}$, $\lambda = 2.02$ Å, the Hamaker constant $H = 6.1 \times 10^{-14}$ erg, and $T = 4$ °C. The expression derived from multilayer data ($T = 25$ °C) by Lis et al. (1982) has been used for V, and eq 1 was solved numerically.

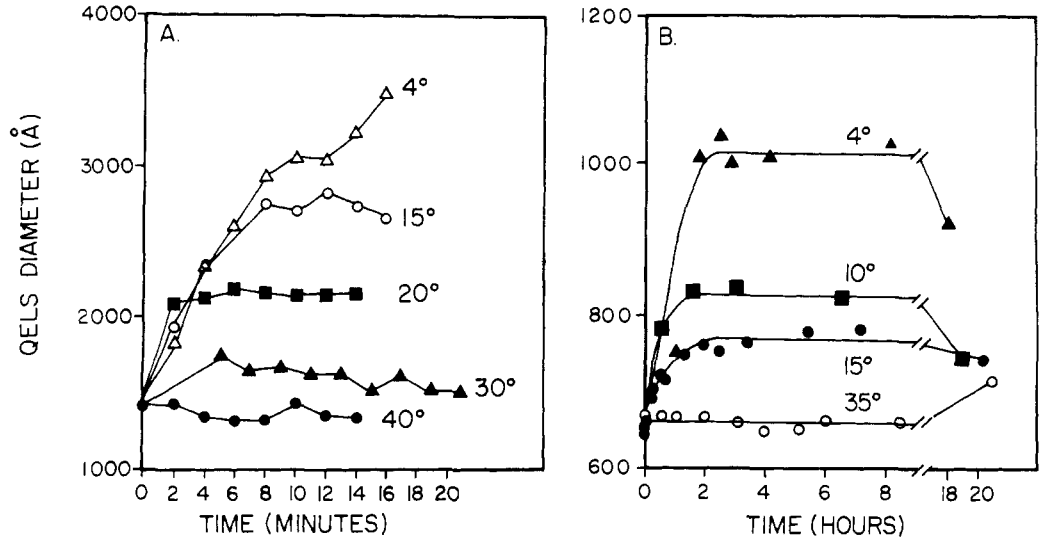

FIGURE 7: QELS diameter as a function of time. Fused vesicles cooled from 50 °C. (A) 950 Å diameter vesicles [3.3 mM (P_i)]. (B) Fractionated 700 Å diameter vesicles [10 mM (P_i)].

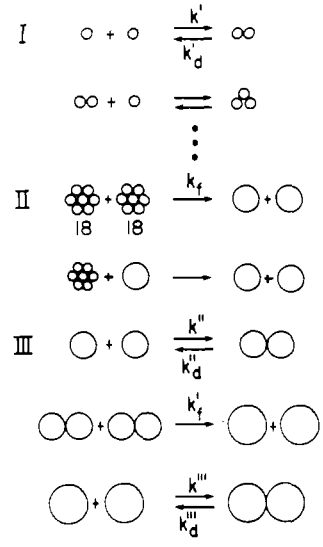

FIGURE 8: Model of DPPC vesicle aggregation and fusion below the phase transition temperature. k', k'', and k''' are the aggregation rate constants. The subscript d denotes disaggregation and f denotes fusion.

than the aggregation rate constant k'.

(II) When the concentration is high and the aggregate size reaches 18, collision between aggregates or between fused vesicles and aggregates causes each aggregate to fuse to a 700 Å diameter vesicle. The number of aggregates containing 18 small vesicles increases with vesicle concentration (Figures 2 and 5), such that the conversion from small to 700 Å diameter vesicles is approximately second order in vesicle concentration (Schmidt et al., 1981; Wong et al., 1982). The size of the fused vesicles is relatively independent of vesicle concentration and temperature which indicates that these variables do not affect the size of the aggregates which fuse. Fused 700-Å vesicles are not the product of collisions between smaller aggregates which sum to 18, since the time course of aggregation, as measured by QELS diameter, is faster than the time course of fusion, as determined by Sepharose CL-2B chromatography. Furthermore, when two aggregates of 18 small vesicles collide, each fuses to form a separate 700-Å vesicle, since the fused vesicle diameter and the maximum QELS diameter are approximately equal (Figure 6).

If the small vesicles are treated as hard spheres, then either cubic closest packing or hexagonal closest packing gives 12 nearest neighbors (6 in the plane, 3 above, and 3 below). Inclusion of next nearest neighbors (3 above and 3 below) gives an aggregate total of 18 arranged around a central vesicle. As aggregate size increases, the total energy of vesicle–vesicle interaction increases and contributes to deformation of the central vesicle. Contributions to deformation are greatest for aggregation of nearest neighbors, less for next nearest neighbors, and small beyond next nearest neighbors. Collisions between aggregates further deform the component vesicles and distribute the deformation throughout the aggregate. Only collisions resulting in large changes in kinetic energy (higher mass aggregates with high relative velocity) sufficiently deform the vesicles to trigger fusion.

At 4 °C, k'_d is small and k_f is less than k', so the overall aggregation–fusion rate is controlled by k_f. At 21 °C, both k' and k_f have increased, but k'_d has increased by a relatively greater amount, decreasing the overall aggregation–fusion rate.

(III) The conversion from 700 Å to 950 Å diameter vesicles is modeled as the aggregation to dimers, followed by the collision between dimers resulting in fusion. Compared to the small vesicle process, 700 Å vesicle aggregation and fusion is slow, requiring about 3 weeks vs. 1 week for small vesicles (4 °C). The rate-limiting step is dimer–dimer collision resulting in fusion. Aggregation is a relatively fast process since dimers are already seen in the QELS diameter curves (Figure 2) after 1 day while 950 Å vesicle formation requires 3–4 weeks of incubation. Interaction between small and 700-Å vesicles is not necessary for conversion to 950-Å vesicles, since pure 700-Å vesicles (Wong et al., 1982). The 950-Å vesicles aggregate, as seen by a gradual increase in the QELS diameter, but fusion to larger vesicles has not been observed after 6 months of incubation.

Acknowledgments

We thank Drs. Adrian Parsegian and Jeffrey Mason for their advice and helpful discussions. We thank Margaretta Allietta for her expert technical assistance in preparing the freeze–fracture electron micrographs.

References

Barenholz, Y., Gibbes, D., Litman, B. J., Goll, J., Thompson, T. E., & Carlson, F. D. (1977) *Biochemistry 16*, 2806.
Bartlett, G. R. (1959) *J. Biol. Chem. 234*, 466.
Briggs, J., & Nicoli, D. F. (1980) *J. Chem. Phys. 72*, 6024.

Chen, S. C., Sturtevant, J. M., & Gaffney, B. J. (1980) *Proc. Natl. Acad. Sci. U.S.A. 77*, 5060.
Chong, C. S., & Colbow, K. (1976) *Biochim. Biophys. Acta 436*, 260.
Day, E. P., Kwok, A. Y. W., Hark, S. K., Ho, J. T., Vail, W. J., Bentz, J., & Nir, S. (1980) *Proc. Natl. Acad. Sci. U.S.A. 77*, 4026.
Derjaguin, B. V. (1935) *Kolloid-Z. 69*, 736.
Fuchs, N. Z. (1934) *Z. Phys. 89*, 736.
Handbook of Physics and Chemistry (1970–1971) 51st ed., CRC Press, Cleveland, OH.
Huang, C. (1969) *Biochemistry 8*, 344.
International Critical Tables (1930) Vol. III, McGraw-Hill, New York.
Jonker, G. H. (1952) in *Colloid Science* (Kruyt, H. R., Ed.) p 94, Elsevier, Amsterdam.
Kerker, M. (1969) in *The Scattering of Light and Other Electromagnetic Radiation*, p 417, Academic Press, New York.
Koppel, D. E. (1972) *J. Chem. Phys. 57*, 4814.
Lansman, J., & Haynes, D. H. (1975) *Biochim. Biophys. Acta 394*, 335.
Le Neveu, D., Rand, R. P., Gingell, D., & Parsegian, V. A. (1977) *Biophys. J. 18*, 209.
Lichtenberg, D., Freire, E., Schmidt, C. F., Barenzholz, Y., Felgner, P. L., & Thompson, T. E. (1981) *Biochemistry 20*, 3462.
Lips, A., Smart, C., & Willis, E. (1971) *Trans. Faraday Soc. 67*, 2979.
Lis, L. J., McAlister, M., Fuller, N., Rand, R. P., & Parsegian, V. A. (1982) *Biophys. J. 37*, 657.
Mason, J. T., & Huang, C. (1978) *Ann. N.Y. Acad. Sci. 308*, 29.
Nir, S., & Bentz, J. (1978) *J. Colloid Interface Sci. 65*, 399.
Nir, S., Bentz, J., & Portis, A. R. (1980) in *Bioelectrochemistry: Ions, Surfaces, Membranes*, p 75, American Chemical Society, Washington, D.C.
Oster, G., & Riley, D. P. (1952) *Acta Crystallogr. 5*, 1.
Ottewill, R. H. (1973) *Colloid Sci. 1*, 173.
Overbeek, J. Th. G. (1952) in *Colloid Science* (Kruyt, H. R., Ed.) p 278, Elsevier, Amsterdam.
Overbeek, J. Th. G. (1977) *J. Colloid Interface Sci. 58*, 408.
Parsegian, V. A., Fuller, N., & Rand, R. P. (1979) *Proc. Natl. Acad. Sci. U.S.A. 76*, 2750.
Schmidt, C. F., Lichtenberg, D., & Thompson, T. E. (1981) *Biochemistry 20*, 4792.
Schullery, S. E., Schmidt, C. F., Felgner, P., Tillack, T. W., & Thompson, T. E. (1980) *Biochemistry 19*, 3919.
Spielman, L. A. (1970) *J. Colloid Interface Sci. 33*, 562.
Suurkuusk, J., Lentz, B. R., Barenholz, Y., Biltonen, R. L., & Thompson, T. E. (1976) *Biochemistry 15*, 1393.
Tinker, D. O. (1972) *Chem. Phys. Lipids 8*, 230.
Verwey, E. J. W., & Overbeek, J. Th. G. (1948) in *Theory of the Stability of Lyophobic Colloids*, Elsevier, Amsterdam.
von Smoluchowski, M. (1917) *Z. Phys. Chem., Stoichiom. Verwandtschaftsl. 92*, 129.
Wiese, G. R., & Healy, T. W. (1970) *Trans. Faraday Soc. 66*, 490.
Wilschut, J., Duzgunes, N., Fraley, R., & Papahadjopoulos, D. (1980) *Biochemistry 19*, 6011.
Wong, M., Anthony, F. H., Tillack, T. W., & Thompson, T. E. (1982) *Biochemistry* (preceding paper in this issue).
Yi, P. N., & MacDonald, R. C. (1973) *Chem. Phys. Lipids 11*, 114.

Reconstitution of the Transferrin Receptor in Lipid Vesicles. Effect of Cholesterol on the Binding of Transferrin†

Marco T. Nunez* and Jonathan Glass

ABSTRACT: Purified rabbit reticulocyte transferrin receptors were incorporated into phosphatidylcholine vesicles containing varying amounts of cholesterol. The binding of transferrin to the receptor in the reconstituted vesicles had three distinct characteristics: (1) The binding of transferrin exhibited the two components characteristic of transferrin binding to erythroid cells, a saturable, specific component and a nonsaturable, nonspecific component. (2) Transferrin binding exhibited positive cooperativity at low cholesterol/phospholipid (C/P) molar ratios. However, the cooperativity diminished and then disappeared as the C/P molar ratios were increased to the levels found in circulating red blood cells. (3) The amount of specific transferrin binding to the reconstituted vesicles also decreased as the C/P molar ratio was increased. These results indicate that in the reconstituted system the lipid environment plays a significant role in the expression of transferrin receptors.

After transferrin binds to its receptor on erythroid cells, a series of still poorly understood events take place which result in the transfer of iron from transferrin to the plasma membrane for transport into the cell and the subsequent release of transferrin to the circulation to undergo another cycle of iron delivery (Jandl & Katz, 1963). The process or transferrin binding and iron release is carried out from the proerythroblast stage of differentiation through that of circulating reticulocytes (Nunez et al., 1977). The reticulocyte undergoes rapid maturation into an erythrocyte upon entering the circulation; simultaneously, the cell loses its ability to bind transferrin. Several hypotheses have been advanced to explain the absence of transferrin binding in mature erythrocytes: (a) the receptor is lost from the cell (VanBockxmeer & Morgan, 1979); (b) the receptor undergoes intrinsic chemical modification that

† From the Charles A. Dana Research Institute and the Harvard-Thorndike Laboratory of the Beth Israel Hospital, Department of Medicine, Beth Israel Hospital and Harvard Medical School, Boston, Massachusetts 02215. *Received December 21, 1981; revised manuscript received March 19, 1982.* Supported by U.S. Public Health Service Grants AM17148 and AM26974. J.G. is a recipient of Research Career and Development Award AM-00513.

0006-2960/82/0421-4139$01.25/0